Inorg. Chem. **2004**, *43*, 7752–7763

Synthesis, Characterization, and Electrochemical Relationships of Dinuclear Complexes of Platinum(II) and Platinum(III) Containing Ortho-Metalated Tertiary Arsine Ligands

Martin A. Bennett,[†,‡] Suresh K. Bhargava,*[,†] Alan M. Bond,[§] Alison J. Edwards,[‡] Si-Xuan Guo,[§] Steven H. Privér,[†] A. David Rae,[‡] and Anthony C. Willis[‡]

School of Applied Sciences (Applied Chemistry), RMIT University, GPO Box 2476V, Melbourne, Victoria 3001, Australia, Research School of Chemistry, Australian National University, Canberra, A.C.T. 0200, Australia, and School of Chemistry, Monash University, PO Box 23, Clayton, Victoria 3800, Australia

Received January 30, 2004

Reaction of 2-Li-4-Me$C_6H_3AsPh_2$ with $[PtCl_2(SEt_2)_2]$ gives two isomeric dinuclear platinum(II) complexes, one containing a half-lantern structure with two chelating and two bridging C_6H_3-5-Me-2-$AsPh_2$ ligands, $[Pt_2(\kappa^2As,C\text{-}C_6H_3\text{-}5\text{-}Me\text{-}2\text{-}AsPh_2)_2(\mu\text{-}\kappa As,\kappa C\text{-}C_6H_3\text{-}5\text{-}Me\text{-}2\text{-}AsPh_2)_2]$, and the other, a full-lantern with four bridging C_6H_3-5-Me-2-$AsPh_2$ ligands, $[Pt_2(\mu\text{-}\kappa As,\kappa C\text{-}C_6H_3\text{-}5\text{-}Me\text{-}2\text{-}AsPh_2)_4]$. The lantern structure of the latter is retained in the dihalodiplatinum(III) complexes that are formed by oxidative addition of chlorine, bromine, or iodine to the isomeric mixture. The dichloro derivative undergoes metathesis reactions with silver or sodium salts, yielding the corresponding cyano, thiocyanato, cyanato, and fluoro species. The structures of all complexes have been determined by single-crystal X-ray analysis. The oxidative addition products have Pt–Pt distances in the range 2.65–2.79 Å (cf. 2.89 Å in the lantern diplatinum(II) structure), consistent with the presence of a Pt–Pt bond. Electrochemical data lead to the conclusion that an initial rapid one-electron process and subsequent chemical reactions produce the dihalodiplatinum(III) lantern structure when mixtures of the lantern and half-lantern complexes are oxidized by halogens. The electrochemical data also explain why chemical reduction of the dihalodiplatinum(III) complex produces only the lantern diplatinum(II) complex.

Introduction

Treatment of 2-$LiC_6H_4PPh_2$ or 2-Li-4-Me$C_6H_3PPh_2$ with $[PtCl_2(SEt_2)_2]$ gives monomeric bis(chelate) complexes $[Pt(\kappa^2P,C\text{-}C_6H_3\text{-}5\text{-}R\text{-}2\text{-}PPh_2)_2]$ (R = H, Me)[1,2] which isomerize slowly in refluxing toluene to the dinuclear species $[Pt_2(\kappa^2P,C\text{-}C_6H_3\text{-}5\text{-}R\text{-}2\text{-}PPh_2)_2(\mu\text{-}\kappa P,\kappa C\text{-}C_6H_3\text{-}5\text{-}R\text{-}2\text{-}PPh_2)_2]$ (Scheme 1).[3] Since there appears to be only one well-authenticated example of a complex containing a four-membered arsenic−carbon chelate ring, $[IrHCl(\kappa^2As,C\text{-}C_6H_4AsPh_2)(AsPh_3)_2]$, which is formed by isomerization of $[IrCl(AsPh_3)_3]$,[4] we were interested to see whether arsenic analogues of the phosphorus monomeric and dimeric species could be made. Unexpectedly, the work has revealed the existence of a novel, lantern-

Scheme 1

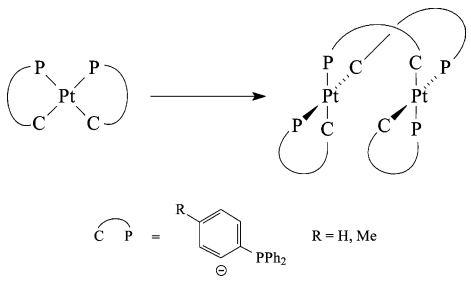

* To whom correspondence should be addressed. E-mail: suresh.bhargava@rmit.edu.au.
† RMIT University.
‡ Australian National University.
§ Monash University.

(1) (a) Bennett, M. A.; Berry, D. E.; Bhargava, S. K.; Ditzel, E. J.; Robertson, G. B.; Willis, A. C. *J. Chem. Soc., Chem. Commun.* **1987**, 1613. (b) Bennett, M. A.; Bhargava, S. K.; Ke, M.; Willis, A. C. *J. Chem. Soc., Dalton Trans.* **2000**, 3537.
(2) Bennett, M. A.; Bhargava, S. K.; Privér, S. H. Unpublished work.
(3) Messelhäuser, J.; Bennett, M. A.; Bhargava, S. K.; Ditzel, E. J.; Robertson, G. B.; Willis, A. C.; Berry, D. E. Presented at the XIIIth International Conference on Organometallic Chemistry, Turin, September 4−9, 1988.
(4) Bennett, M. A.; Milner, D. L. *J. Am. Chem. Soc.* **1969**, *91*, 6983.

10.1021/ic0498790 CCC: $27.50
Published on Web 10/28/2004

Scheme 2

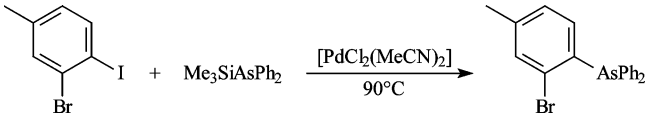

shaped diplatinum(II) complex that contains only bridging As,C ligands, whose P,C-analogue has never been detected. Oxidative addition of halogens affords dihalodiplatinum(III) complexes that retain the lantern structure, and electrochemical studies have enabled some of the mechanistic details of the reactions to be elucidated.

Results

Ligand Synthesis. Since there is no convenient probe analogous to ^{31}P NMR spectroscopy available for tertiary arsine complexes, we chose to study compounds derived from the reagent 2-Li-4-Me$C_6H_3AsPh_2$ containing a useful ^{1}H NMR indicator group. The required precursor, 2-Br-4-Me$C_6H_3AsPh_2$, can be obtained by the reaction of 2-Br-4-Me$C_6H_3AsCl_2$ with PhMgBr, following the literature procedure for the preparation of 2-Br$C_6H_4AsPh_2$ from 2-BrC_6H_4-$AsCl_2$.[5] A convenient alternative, which avoids the synthesis of the dichloroarsine from 2-bromo-4-methylaniline, employs the $[PdCl_2(MeCN)_2]$-catalyzed reaction of 3-bromo-4-iodotoluene with (trimethylsilyl)diphenylarsine (Scheme 2); the latter reagent is easily prepared in high yield from the reaction of Me_3SiCl with $LiAsPh_2$.[6] It is worth noting that the reaction of Scheme 2 is complete after ca. 2 h at 90 °C, whereas the corresponding reaction of 2-BrC_6H_4I with Me_3-$SiPPh_2$ is reported to require 100 h at 70 °C.[7]

Platinum(II) Complexes. The reaction of 2-Li-4-MeC_6H_3-$AsPh_2$ with $[PtCl_2(SEt_2)_2]$ in ether at −30 °C gave a yellow solid with the empirical formula $[Pt(MeC_6H_3AsPh_2)_2]$ in ca. 40% yield (Scheme 3). The ^{1}H NMR spectrum in the aromatic methyl region showed a pair of equally intense singlets at δ 1.93 and 1.98 accompanied by a singlet at δ 2.18 of approximately the same intensity, thus suggesting the presence of at least two species. Slow crystallization from CH_2Cl_2/MeOH afforded crystals of two distinct compounds, which were shown by X-ray crystallography to be isomeric dinuclear platinum(II) complexes. As shown in Figure 1, the major isomer **1** is structurally similar to its phosphorus analogue; two of the C_6H_3-5-Me-2-$AsPh_2$ groups behave as chelate ligands, while the other two bridge the metal atoms.

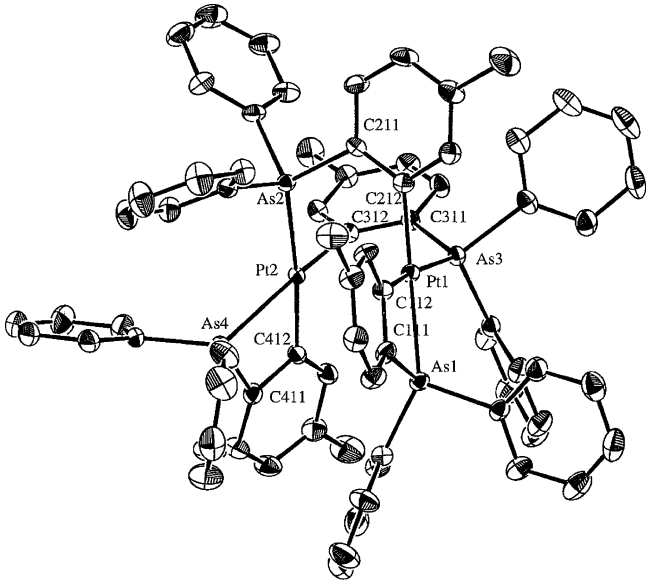

Figure 1. Molecular structure of $[Pt_2(\kappa^2As,C\text{-}C_6H_3\text{-}5\text{-}Me\text{-}2\text{-}AsPh_2)_2(\mu\text{-}\kappa As,\kappa C\text{-}C_6H_3\text{-}5\text{-}Me\text{-}2\text{-}AsPh_2)_2]$ (**1**). Ellipsoids show 30% probability levels. Hydrogen atoms have been deleted for clarity.

We refer to this as a half-lantern structure. In contrast, in the minor isomer **2**, all four C_6H_3-5-Me-2-$AsPh_2$ groups span the platinum atoms to give a lantern-type structure (Figure 2) that is similar in basic geometry to $[Pt_2(pop)_4]^{4-}$ (pop = μ-*P,P*-pyrophosphite, $P_2O_5H_2^{2-}$)[8] and to many platinum(II) dimers containing the donor atom sets S−S and N−S.[9] Both isomers exhibit strong green−yellow luminescence in the solid state under UV irradiation. In contrast to the phosphorus-based system,[1,2] no evidence was found for a monomeric species $[Pt(\kappa^2As,C\text{-}C_6H_3\text{-}5\text{-}Me\text{-}2\text{-}AsPh_2)_2]$.

In the ^{1}H NMR spectrum of the mixture, the singlet at δ 2.18 is assigned to the methyl protons of the equivalent bridging C_6H_3-5-Me-2-$AsPh_2$ groups of **2**, while the singlets at δ 1.93 and 1.98 belong to the inequivalent C_6H_3-5-Me-2-$AsPh_2$ groups of **1**. It is not known which corresponds to the chelate and which to the bridging ligands. The ratio of **1** to **2** in typical preparations was ca. 2:1, as estimated by integration, although heating the mixture in refluxing toluene caused complete conversion into **2**. The ^{1}H NMR spectrum of the mixture also shows a 4H singlet at δ 7.90 with ^{195}Pt satellites (J_{Pt-H} = 58.4 Hz), which is well separated from the other aromatic multiplets and can be assigned to the aromatic protons ortho to the Pt−C bond. Coupling constants

Scheme 3

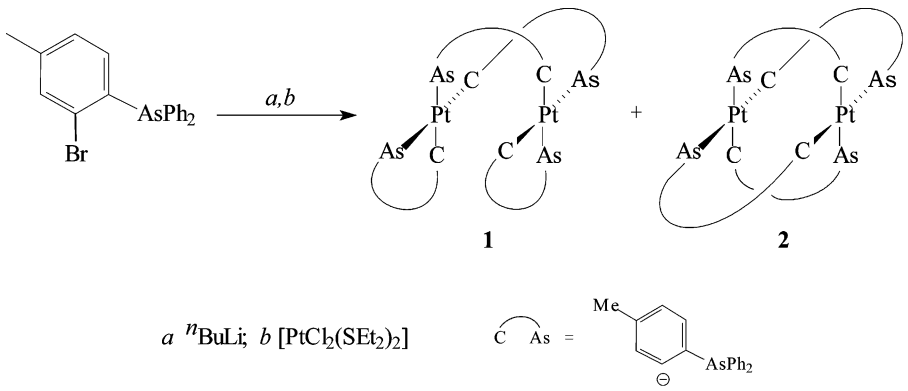

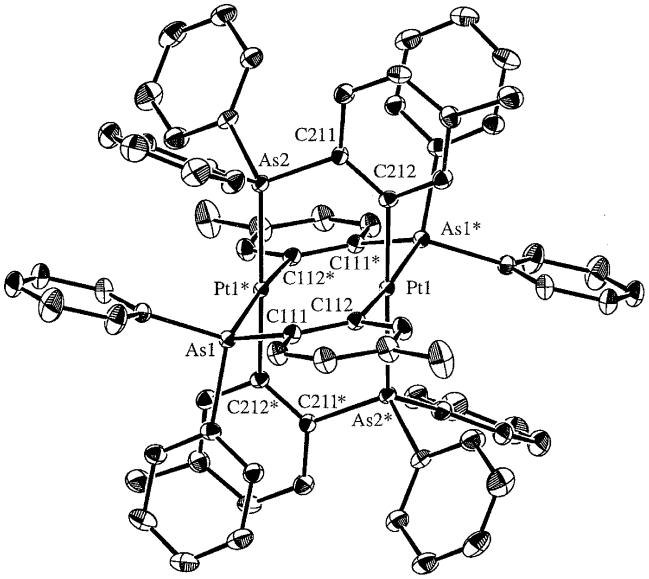

Figure 2. Molecular structure of $[Pt_2(\mu\text{-}\kappa As,\kappa C\text{-}C_6H_3\text{-}5\text{-}Me\text{-}2\text{-}AsPh_2)_4]$ **(2)**. Ellipsoids show 30% probability levels. Hydrogen atoms have been deleted for clarity. Asterisks denote atoms related by inversion symmetry.

of a similar magnitude have been reported for the ortho-proton of a η^1-C_6H_4 group in cycloplatinated complexes containing deprotonated 6-(1-methylbenzyl)-2,2′-bipyridine, e.g., $[PtCl\{2\text{-}C_6H_4(CHMe)C_5H_3NC_5H_4N\}]$.[10] The fast atom bombardment (FAB) mass spectrum of the mixture shows a parent-ion peak corresponding to the dimer. The structures of **1** and **2** are discussed in more detail below.

Platinum(III) Complexes. Addition of iodobenzene dichloride to a mixture of isomers **1** and **2** in CH_2Cl_2 gave quantitatively an orange solid which showed only one methyl ^{1}H NMR signal at δ 2.19 and a 4H singlet at δ 8.32 with ^{195}Pt satellites (J_{Pt-H} = 35.0 Hz) assignable to the ortho-aromatic protons. Structural analysis of a crystal obtained from CH_2Cl_2/MeOH showed the compound to be the platinum(III)−platinum(III) lantern complex $[Pt_2Cl_2(\mu\text{-}\kappa As,\kappa C\text{-}C_6H_3\text{-}5\text{-}Me\text{-}2\text{-}AsPh_2)_4]$ (**3**) derived by oxidative addition of chlorine across the dinuclear unit of **2** (Scheme 4); the same compound also formed over a period of days from a solution of **1** and **2** in CH_2Cl_2 and, more rapidly, in $CHCl_3$ or CCl_4. Complex **1** evidently isomerizes under the reaction conditions (probably via $\mathbf{1}^+$, according to the electrochemical studies), leading to **3** as the sole product. Zinc dust reduction of **3** regenerates **2** free from **1**.

The corresponding complexes $[Pt_2X_2(\mu\text{-}\kappa As,\kappa C\text{-}C_6H_3\text{-}5\text{-}Me\text{-}2\text{-}AsPh_2)_4]$ (X = Br (**4**), I (**5**)) were obtained similarly

Scheme 4

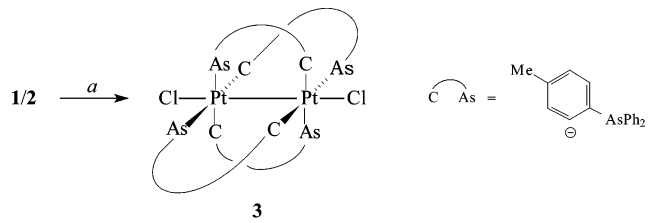

a $PhICl_2$ or CH_2Cl_2

Table 1. Aromatic Methyl and Ortho-Proton ^{1}H NMR Data for Diplatinum(II) and Diplatinum(III) Complexes of the Type $[Pt_2X_2(\mu\text{-}\kappa As,\kappa C\text{-}C_6H_3\text{-}5\text{-}Me\text{-}2\text{-}AsPh_2)_4]$[a]

X···X	δ (Me)	δ (H_{ortho}) ($^3J_{Pt-H}$)
X absent in (**2**)	2.18	7.90 (58.4)
Cl···Cl (**3**)	2.19	8.32 (35.0)
Br···Br (**4**)	2.16	8.49 (37.9)
I···I (**5**)	2.12	8.90 (42.8)
NC···CN (**6**)	2.23	8.60 (46.9)
SCN···NCS (**7**)	2.22	7.79 (37.7)
OCN···NCO (**8**)	2.17	7.90 (37.4)
F···F (**9**)[b]	2.18	8.04 (29.4)

[a] In $CDCl_3$. [b] In CD_2Cl_2.

to **3** as brick red and purple solids, respectively, by addition of bromine or iodine to complex **2**. Similar oxidative additions are known for other diplatinum(II) lantern complexes.[8,9] Both compounds can also be obtained by anion exchange from **3**. Methyl iodide reacted over a period of days with a solution of **2** in the dark to give **5**; in laboratory light the reaction was complete in 2−3 h. The highest mass peak in the FAB mass spectra of **3**−**5** corresponds to the loss of one halide ion. A strong band at 203 cm^{-1} in the IR spectrum of **3** may be due to ν(PtCl), but the assignment is tentative because there is strong ligand absorption in the region of 500−150 cm^{-1}.

Treatment of **3** with AgCN, NaSCN, NaNCO, or AgF gave the corresponding dicyano-, bis(thiocyanato)-, bis(cyanato)-, and difluorodiplatinum(III) complexes $[Pt_2X_2(\mu\text{-}\kappa As,\kappa C\text{-}C_6H_3\text{-}5\text{-}Me\text{-}2\text{-}AsPh_2)_4]$ (X = CN (**6**), NCS (**7**), NCO (**8**), and F (**9**)) as yellow solids, which were identified on the basis of single-crystal X-ray studies (see below) and spectroscopic data. The highest peak in the electron ionization (EI) mass spectra of **6**−**8** corresponds to the loss of one anion while the parent ion was observed for **9**. The solid-state IR spectra of **6**−**8** each show a ν(CN) band in the 2100−2200 cm^{-1} region. In the case of **7**, the broad ν(CN) band at 2086 cm^{-1} is suggestive of N-bonded thiocyanate, a feature that is confirmed by the X-ray diffraction study (see below). Criteria based on ν(CS), δ(NCS), or ν(M-NCS)[11] could not be applied because of numerous overlapping bands in the appropriate regions.

The ^{1}H NMR spectra of complexes **4**−**9** show the characteristic ^{195}Pt-coupled resonance for the ortho proton in the region of δ 8 (see Table 1), the magnitude of $^3J_{Pt-H}$ (29.4−46.9 Hz) being ca. $^2/_3$ of that observed in the diplatinum(II) precursor **2**. A similar relationship holds for

(5) (a) Jones, E. R. H.; Mann, F. G. *J. Chem. Soc.* **1955**, 4472. (b) Cochran, W.; Hart, F. A.; Mann, F. G. *J. Chem. Soc.* **1957**, 2818. (c) Levason, W.; McAuliffe, C. A. *Inorg. Synth.* **1976**, *16*, 184. (d) Talay, R.; Rehder, W. *Z. Naturforsch., B: Chem. Sci.* **1981**, *36*, 451.
(6) Fenske, D.; Teichert, H.; Pokscha, H.; Renz, W.; Becher, H. *Monatsh. Chem.* **1980**, *111*, 177.
(7) Tunney, S. E.; Stille, J. K. *J. Org. Chem.* **1987**, *52*, 748.
(8) (a) Zipp, A. P. *Coord. Chem. Rev.* **1988**, *84*, 47. (b) Roundhill, D. M.; Gray, H. B.; Che, C. M. *Acc. Chem. Res.* **1989**, *22*, 55. (c) Sweeney, R. J.; Harvey, E. L.; Gray, H. B. *Coord. Chem. Rev.* **1990**, *105*, 23.
(9) (a) Woollins, J. D.; Kelly, P. F. *Coord. Chem. Rev.* **1985**, *65*, 115. (b) Umakoshi, K.; Sasaki, Y. *Adv. Inorg. Chem.* **1994**, *40*, 187.
(10) Romeo, R.; Plutino, M. R.; Scolaro, L. M. *Inorg. Chim. Acta* **1997**, *265*, 225.
(11) Nakamoto, K. *Infrared and Raman Spectra of Inorganic and Coordination Compounds*, 5th ed.; John Wiley: New York, 1997; Part B, pp 116−121.

$^1J_{Pt-P}$ in the diplatinum(II) complexes, $[Pt_2(pop)_4]^{4-}$ and $[Pt_2(pcp)_4]$,$^{4-}$ and their oxidative addition products, $[Pt_2X_2(pop)_4]^{4-}$ and $[Pt_2X_2(pcp)_4]^{4-}$ (pcp = $[CH_2\{P(O)OH\}_2]^{2-}$).[12] In the case of planar platinum(II) and octahedral platinum(IV) complexes, PtX_2L_2 and PtX_4L_2, the corresponding trend in coupling constants such as $^1J_{Pt-P}$ and $^2J_{Pt-CH_3}$ is generally attributed to the change in s-character of the Pt−L bonding orbital in the two oxidation states.[13,14] The magnitude of $^3J_{Pt-H}$ in complexes **3**−**9** is also sensitive to the nature of the axial ligand X, ranging from 29.4 Hz (X = F) and 35.0 Hz (X = Cl) to 42.8 Hz (X = I) and 46.9 Hz (X = CN).

The presence of a covalent Pt−F bond in complex **9** was confirmed by the ^{19}F NMR spectrum in CD_2Cl_2, which shows a singlet at δ −228.6 with two sets of ^{195}Pt satellites ($^1J_{Pt-F}$ = 492 Hz, $^2J_{Pt-F}$ = 192 Hz). The NMR parameters are comparable with those of the few well-characterized fluoroplatinum complexes, the $^1J_{Pt-F}$ values being intermediate between those reported for Pt(II) and Pt(IV); cf. $[Pt^{II}F(PEt_3)_3]BF_4$ (250 Hz),[15] *trans*-$[Pt^{II}F(PEt_3)_2(PPh_3)]ClO_4$ (215 Hz),[16] *trans*-$[Pt^{II}PhF(PPh_3)_2]$ (399 Hz),[17] and $[Me_3Pt^{IV}F]_4$ (708 Hz).[18]

There was no evidence for the formation of a mixed oxidation state complex $[Pt_2^{II,III}Cl(\mu\text{-}\kappa As,\kappa C\text{-}C_6H_3\text{-}5\text{-}Me\text{-}2\text{-}AsPh_2)_4]$ from solutions of equimolar amounts of **2** and **3**. Attempts to prepare a thiocyanato Pt_2(II,III) species from solutions of **2** and **7** also failed. In contrast, linear chain Pt_2(II,III) complexes of pop and dithioacetate, $K_4[Pt_2X(pop)_4]$ (X = Cl, Br, I) and $[Pt_2I(S_2CMe)_4]$ are readily formed.[8b,9] The aromatic rings of the bulky $AsPh_2$ groups possibly hinder bridging of halide or thiocyanate between pairs of dimeric units.

In an effort to prepare sterically less hindered complexes containing $\mu\text{-}\kappa As,\kappa C\text{-}C_6H_4\text{-}2\text{-}AsMe_2$, we treated $2\text{-}LiC_6H_4\text{-}AsMe_2$ with $[PtCl_2(SEt_2)_2]$. Analysis of the resulting orange−yellow solid showed the expected formulation, $[Pt(C_6H_4\text{-}AsMe_2)_2]$ (**10**), but its ^{1}H NMR spectrum at 23 °C showed broad multiplets for the aromatic and $AsMe_2$ resonances that did not sharpen when the solution was cooled to −80 °C. Treatment of **10** with $PhICl_2$ gave the expected oxidative addition product, $[Pt_2Cl_2(C_6H_4AsMe_2)_4]$ (**11**) as an orange solid whose ^{1}H NMR spectrum also showed broad aromatic and $AsMe_2$ resonances. Both **10** and **11** appeared to be dimeric in ca. 0.2 M CH_2Cl_2 solution by vapor pressure osmometry, but we could not obtain satisfactory mass spectra or crystals adequate for an X-ray diffraction study. We suspect that **10** and **11** may consist of a mixture of rapidly interconverting oligomers in solution.

X-ray Crystallographic Determinations. The structures of the isomeric diplatinum(II) complexes **1** and **2** are shown in Figures 1 and 2; selected bond lengths and angles are listed in Tables S1 and S2, respectively. In both complexes the coordinated arsenic atoms are mutually cis. The coordination geometry about each metal atom is close to planar in **2** but that in **1** is more distorted. The small bite angle of the four-membered rings in **1** (69.7(3)° (av)) is similar to that of many $\kappa^2P,C\text{-}C_6H_4\text{-}2\text{-}PPh_2$ complexes[19] and is associated with a widening of the As−Pt−As angles to ca. 106°. Corresponding metal−ligand bond lengths in the bridging groups of **1** and **2** and the chelate groups of **1** do not differ significantly. As expected, the Pt−As bond lengths in **1** and **2** are ca. 0.15 Å greater than the Pt−P bond lengths in $[Pt_2(\kappa^2P,C\text{-}C_6H_4\text{-}2\text{-}PPh_2)_2(\mu\text{-}\kappa P,\kappa C\text{-}C_6H_4\text{-}2\text{-}PPh_2)_2]$, although the Pt···Pt separation in **1** (3.4208(3) Å) is only slightly greater than that in $[Pt_2(\kappa^2P,C\text{-}C_6H_4\text{-}2\text{-}PPh_2)_2(\mu\text{-}\kappa P,\kappa C\text{-}C_6H_4\text{-}2\text{-}PPh_2)_2]$ (3.3875(4) Å).[3] The shorter Pt···Pt separation in **2** (2.8955(4) Å) is presumably a consequence of the four bridging groups; it falls between those observed in similar lantern structures containing N−S or S−S bridging groups such as 4-methylpyridine-2-thiolate and dithiocarboxylates (2.68 Å and 2.76−2.86 Å, respectively) on one hand and P−P bridging groups such as pop (2.92−2.98 Å) on the other.[8,9]

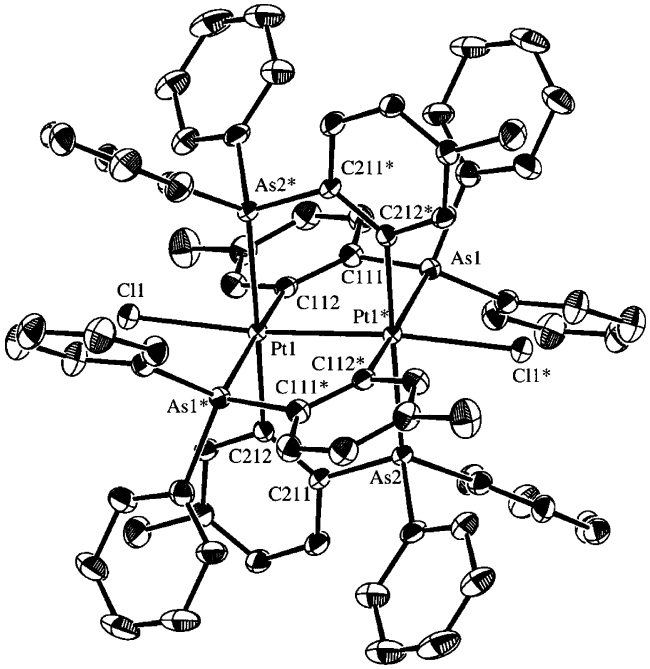

Figure 3. Molecular structure of $[Pt_2Cl_2(\mu\text{-}\kappa As,\kappa C\text{-}C_6H_3\text{-}5\text{-}Me\text{-}2\text{-}AsPh_2)_4]$ **(3)**.[20] Ellipsoids show 30% probability levels. Hydrogen atoms have been deleted for clarity. Asterisks denote atoms related by inversion symmetry.

The diplatinum(III) complexes **3**−**9** all have similar lantern structures[20] derived from addition of a pair of halide or

(12) King, C.; Roundhill, D. M.; Dickson, M. K.; Fronczek, F. R. *J. Chem. Soc., Dalton Trans.* **1987**, 2769.
(13) Pregosin, P. S.; Kunz, R. W. *^{31}P and ^{13}C NMR of Transition Metal Phosphine Complexes*; Springer: Berlin, 1979; p 23
(14) Appleton, T. G.; Clark, H. C.; Manzer, L. E. *Coord. Chem. Rev.* **1973**, *10*, 335 and references therein.
(15) Dixon, K. R.; McFarland, J. J. *J. Chem. Soc., Chem. Commun.* **1972**, 1274.
(16) Cairns, M. A.; Dixon, K. R.; McFarland, J. J. *J. Chem. Soc., Dalton Trans.* **1975**, 1159.
(17) Nilsson, P.; Plamper, F.; Wendt, O. F. *Organometallics* **2003**, *22*, 5235.
(18) Cross, R. J.; Haupt, M.; Rycroft, D. S.; Winfield, J. M. *J. Organomet. Chem.* **1999**, *587*, 195.
(19) For platinum(II), see: (a) Clark, H. C.; Hine, K. E. *J. Organomet. Chem.* **1976**, *105*, C32. (b) Rice, N. C.; Oliver, J. D. *J. Organomet. Chem.* **1978**, *145*, 121. (c) Scheffknecht, C.; Rhomberg, A.; Müller, E. P.; Peringer, P. *J. Organomet. Chem.* **1993**, *463*, 245. (d) Clark, H. C. S.; Fawcett, J.; Holloway, J. H.; Hope, E. G.; Peck, L. A.; Russell, D. R. *J. Chem. Soc., Dalton Trans.* **1998**, 1249. (e) Bennett, M. A.; Dirnberger, T.; Hockless, D. C. R.; Wenger, E.; Willis, A. C. *J. Chem. Soc., Dalton Trans.* **1998**, 271. (f) Bennett, M. A.; Berry, D. E.; Dirnberger, T.; Hockless, D. C. R.; Wenger, E. *J. Chem. Soc., Dalton Trans.* **1998**, 2367. (g) Bender, R.; Bouaoud, S.-E.; Braunstein, P.; Dusausoy, F.; Merabet, N.; Raya, J.; Rouag, D. *J. Chem. Soc., Dalton Trans.* **1999**, 735.

Table 2. Crystal and Refinement Data for Complexes **1**−**9**

	1	**2**	**3**	**4**	**5**
formula	$C_{76}H_{64}As_4Pt_2 \cdot 1.5CH_2Cl_2$	$C_{76}H_{64}As_4Pt_2 \cdot 2CH_2Cl_2$	$C_{76}H_{64}As_4Cl_2Pt_2 \cdot 4CH_2Cl_2$	$C_{76}H_{64}As_4Br_2Pt_2 \cdot 4CH_2Cl_2$	$C_{76}H_{64}As_4I_2Pt_2 \cdot 2CH_2Cl_2$
fw	1794.61	1837.05	2077.85	2166.62	2090.88
crystal system	triclinic	monoclinic	triclinic	triclinic	monoclinic
space group	$P\bar{1}$	$P2_1/n$	$P\bar{1}$	$P\bar{1}$	$P2_1/c$
a, Å	12.0083(1)	11.8523(1)	12.5394(2)	12.5730(1)	13.9842(1)
b, Å	12.9967(1)	19.3514(2)	12.7062(2)	12.7721(1)	13.0891(1)
c, Å	23.1465(2)	14.8829(2)	13.5404(3)	13.5519(1)	39.8723(3)
α, deg	91.6097(3)		97.7853(9)	97.4468(5)	
β, deg	96.7525(3)	105.9379(5)	98.1840(10)	98.2516(6)	91.6151(3)
γ, deg	110.253(4)		115.2438(9)	115.0814(4)	
V, Å^3	3356.45(5)	3282.3	1884.53(6)	1906.5(3)	7295.35(9)
Z	2	2	1	1	4
color, habit	yellow block	green rod	orange needle	red block	black needle
cryst dimens (mm)	0.40 × 0.26 × 0.14	0.37 × 0.11 × 0.07	0.16 × 0.09 × 0.05	0.25 × 0.20 × 0.18	0.33 × 0.04 × 0.04
D_{calc} (g cm^{-3})	1.776	1.859	1.831	1.888	1.904
μ (mm^{-1})	6.283	6.6467	5.85	6.761	6.67
no. indep reflns (R_{int})	15358 (0.047)	9585 (0.063)	8655 (0.057)	11150 (0.039)	12843 (0.09)
no. of obsd refln [$I > 3\sigma(I)$]	9237	5141	4906	9053	10083
no. of params refined	784	393	433	434	277
R(F)	0.026	0.027	0.032	0.035	0.039
R_w(F)	0.028	0.029	0.036	0.040	0.054
ρ_{max}/ρ_{min} (e Å^{-3})	0.59/-0.83	1.06/-1.30	0.88/-1.07	2.05/-3.28	1.65/-1.59

	6	**7**	**8**	**9**
formula	$C_{78}H_{64}As_4N_2Pt_2 \cdot 4CH_2Cl_2$	$C_{78}H_{64}As_4N_2Pt_2S_2$	$C_{78}H_{64}As_4N_2O_2Pt_2 \cdot 2CH_2Cl_2$	$2[C_{76}H_{64}As_4F_2Pt_2] \cdot CH_2Cl_2 \cdot H_2O$
fw	2058.98	1783.38	1921.11	3513.36
crystal system	triclinic	monoclinic	monoclinic	monoclinic
space group	$P\bar{1}$	$C2/c$	$P2_1/c$	$P2_1/n$
a, Å	12.5155(1)	27.1169(3)	13.8368(1)	26.1349(1)
b, Å	12.7912(1)	17.9852(3)	13.0378(1)	12.9746(1)
c, Å	13.5105(2)	17.0499(3)	40.5832(2)	38.4786(3)
α, deg	97.6692(5)			
β, deg	98.6654(5)	97.1223(6)	91.1694(2)	94.3806(2)
γ, deg	114.1778(5)			
V, Å^3	1904.15(4)	6425.44(18)	7319.74	13009.59(15)
Z	1	4	4	4
color, habit	yellow plate	yellow needle	yellow plate	yellow plate
cryst dimens (mm)	0.30 × 0.20 × 0.19	0.36 × 0.05 × 0.05	0.44 × 0.07 × 0.03	0.26 × 0.11 × 0.03
D_{calc} (g cm^{-3})	1.795	1.843	1.743	1.793
μ (mm^{-1})	5.721	6.507	5.807	6.407
no. indep reflns (R_{int})	8746 (0.05)	7358 (0.06)	12849 (0.037)	23024 (0.07)
no. of obsd refln [$I > 3\sigma(I)$]	7137	4143	9512	12068[a]
no. of params refined	453	397	839	1559
R(F)	0.023	0.022	0.024	0.027
R_w(F)	0.025	0.025	0.026	0.027
ρ_{max}/ρ_{min} (e Å^{-3})	0.84/-0.87	0.90/-0.81	1.07/-0.89	0.79/-0.89

[a] [$I \geq 2\sigma(I)$].

pseudohalide groups along the axis of **2**. The structure of the dichloro complex **3** is shown in Figure 3. Selected bond lengths and angles in complexes **3**, **4**, **6,** and **7** are listed in Table S2; those for complexes **5**, **8**, and **9** are given in Table S3. As is evident from the crystal and refinement data in Table 2, the CH_2Cl_2 solvates of the dichloro, dibromo, and dicyano complexes, **3**, **4,** and **6**, are isomorphous (space group $P\bar{1}$, $Z = 1$), as are the CH_2Cl_2-solvated diiodo- and bis(cyanato)-complexes **5** and **8** (space group $P2_1/c$, $Z = 4$). In contrast, the bis(thiocyanato) complex **7** is not solvated by CH_2Cl_2 and belongs to a different space group ($C2/c$, $Z = 4$), while two molecules of the difluoro complex (**9a** and **9b**) ($P2_1/n$, $Z = 4$) are associated with one CH_2Cl_2 molecule and one water molecule (the basis of the identification is further discussed in Appendix S1). The Pt−Pt distances in **3**−**9** depend on the nature of the axial ligand X and are significantly shorter than that in the parent complex **2**, consistent with the presence of a discrete single bond between the $5d^7$ metal centers.

The Pt−Pt distances are shortest for the difluoride **9** (**9a**, 2.6530(4) Å; **9b**, 2.6524(4) Å) and for complexes **7** and **8** containing N-bonded NCS and NCO (2.6870(3), 2.6772(2) Å, respectively) and longest for the C-bonded dicyano complex **6** (2.7910(2) Å). A similar trend can be seen in the diplatinum(III) complexes containing pop; the shortest Pt−Pt distance occurs in the N-donor acetonitrile complex $[^nBu_4N]_2[Pt_2(pop)_4(NCMe)_2]$ (2.676(1) Å),[21] while the longest

(20) The metal−metal vectors are generally not exactly perpendicular to the plane of the Pt and the four attached atoms, as can be seen from the range of metal−metal attached atom angles in Tables S2 and S3.

(21) Che, C. M.; Mak, T. C. W.; Miskowski, V. M.; Gray, H. B. *J. Am. Chem. Soc.* **1986**, *108*, 7840.

occurs in the methyl iodide oxidative addition product $K_4[Pt_2(I)(Me)(pop)_4]\cdot 2H_2O$ (2.782(1) Å).[22] The distances in the dihalo complexes are essentially equal for the dichloride (**3**) and dibromide (**4**) (2.7444(5) and 2.7457(1) Å, respectively) and are slightly greater in the diiodide (**5**) (2.752(1) Å); they are also similar to the Pt−Pt distances in corresponding lantern complexes derived from pop and pcp, e.g., 2.7500(3) Å in $K_4[Pt_2Cl_2(pcp)_4]\cdot 8H_2O$ (**12**),[12] 2.695(1) Å in $K_4[Pt_2Cl_2(pop)_4]\cdot 2H_2O$ (**13**),[23] 2.723(4) Å in $K_4[Pt_2Br_2(pop)_4]\cdot 2H_2O$ (**14**),[24] 2.716(1) Å in $[^nBu_4N]_4[Pt_2Br_2(pop)_4]$ (**15**),[25] 2.754(1) Å in $K_4[Pt_2I_2(pop)_4]\cdot 2H_2O$ (**16**),[25] and 2.742(1) Å in $K_2[^nBu_4N]_2[Pt_2I_2(pop)_4]$ (**17**).[25]

The Pt−halide distances in **3**−**5** and **9** are ca. 0.15−0.20 Å longer than the distances found in $[PtX_6]^{2-}$, reflecting the high trans-influence of the Pt−Pt bond. The Pt−Cl distance in **3** (2.4884(16) Å) is also significantly greater than those in **12** (2.442(1) Å)[16] or **13** (2.407(2) Å),[23] perhaps reflecting the greater bulk and stronger electron-donating ability of the bridging As−C ligand relative to those of pop. There is a similar trend in the Pt−I distances (**5**, 2.779(1) Å; **16**, 2.742(1) Å;[25] **17**, 2.721(1) Å[25]). Complex **9** is unique in that there are no analogous lantern-type dimers containing terminal fluoride ligands; an unsupported dimer containing α-dioximato ligands has been reported,[26] although no characterization details are given. The Pt−F distances (see Table S3) in **9** (**9a**, 2.139(4), 2.100(4) Å; **9b**, 2.172(5), 2.128(4) Å for the two independent molecules in the asymmetric unit) lie in the range found for the platinum(II) salt $[PtF(PEt_3)_3]BF_4$ (2.043(7) Å)[27] and the platinum(IV) complex $[PtMe_3F]_4$ (2.251(6) Å)[18] in which fluoride is trans to a ligand of high trans-influence; the Pt−F distances in platinum(IV) complexes containing mutually *trans*-fluorides are much shorter, e.g. 1.930(2) Å in *trans*-$[^nBu_4N]_2[PtF_2(C_2O_4)_2]$[28] and 1.938(10), 1.943(10) Å in *trans*-$[PtF_2(py)_4][BF_4]_2\cdot H_2O$.[29]

Crystalline **7** and **8** contain N-bonded thiocyanate and cyanate, respectively; in both cases, as commonly observed in mononuclear complexes of these ligands, the Pt−N−C bond angles deviate markedly from linearity (**7**, 164.8(4)°; **8**, 146.2(3)°, 166.1(5)°). In contrast to **7**, the pop analogue contains S-bonded thiocyanate in the solid state.[30] The Pt−N distances in **7** and **8**, and the Pt−C distances in **6**, are all longer than those found in typical cyanato-, thiocyanato-, and cyano-platinum(II) complexes, respectively, again reflecting the high trans-influence of the Pt−Pt bond. The Pt−As and Pt−C distances in the diplatinum(II) complexes **1** and **2** are, separately, not significantly different (ca. 2.43−2.47 Å, 2.02−2.05 Å, respectively). Oxidative addition to form the diplatinum(III) complexes **3**−**9** produces little effect on the Pt−As distances but does lead to a significant lengthening in the Pt−C distances to ca. 2.10−2.13 Å.

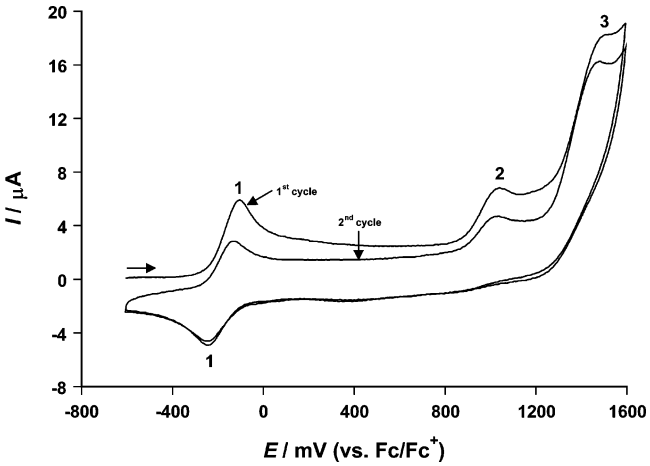

Figure 4. Cyclic voltammogram obtained for oxidation of a 1.0 mM solution of complex **2** at a 1 mm diameter GC working electrode in dichloromethane (0.1 M Bu_4NPF_6) at a scan rate of 1000 mV s^{-1}.

Electrochemical Oxidation of $[Pt_2(\mu\text{-}\kappa As,\kappa C\text{-}C_6H_3\text{-}5\text{-}Me\text{-}2\text{-}AsPh_2)_4]$ (2). Three processes are detected for the voltammetric oxidation of **2** in dichloromethane (0.1 M Bu_4NPF_6). The first process, labeled 1 in Figure 4, is chemically and electrochemically reversible with a reversible formal potential (E_f^0) of −165 ± 5 mV vs Fc/Fc^+ at both glassy carbon and platinum disk electrodes. This process is assigned[31] to the structurally conserved $\mathbf{2}^{0/+}$ couple (eq 1).

$$[Pt_2(\mu\text{-}\kappa As,\kappa C\text{-}C_6H_3\text{-}5\text{-}Me\text{-}2\text{-}AsPh_2)_4] \rightleftharpoons [Pt_2(\mu\text{-}\kappa As,\kappa C\text{-}C_6H_3\text{-}5\text{-}Me\text{-}2\text{-}AsPh_2)_4]^+ + e^- \quad (1)$$

The second and third oxidation processes (labeled 2 and 3 in Figure 4) are irreversible and have peak potentials (E_p^{ox}) near 1.0 and 1.5 V vs Fc/Fc^+. The irreversibility suggests that a gross structural change accompanies more extensive oxidation to a diplatinum(III) complex. The overall reaction scheme is consistent with eq 2.

$$[Pt_2(II,II)] \underset{+e^-}{\overset{-e^-}{\rightleftharpoons}} [Pt_2(II,III)]^+ \underset{+e^-}{\overset{-e^-}{\rightleftharpoons}} [Pt_2(III,III)]^{2+} \rightarrow \text{electroactive product} \quad (2)$$

Cyclic voltammograms obtained after a one-electron bulk oxidative electrolysis of **2** at a platinum electrode using a controlled potential of +170 mV vs Fc/Fc^+ (between processes 1 and 2) exhibit exactly the same three processes shown in Figure 4. However, while processes 2 and 3 remain oxidative, reversible process 1 is now reductive and corresponds to the reaction $\mathbf{2}^{+/0}$ instead of $\mathbf{2}^{0/+}$ as was the case prior to bulk electrolysis. Thus, a stable lantern $\mathbf{2}^+$ species exists on the voltammetric and bulk electrolysis time scales

(22) Che, C. M.; Mak, T. C. W.; Gray, H. B. *Inorg. Chem.* **1984**, *23*, 4386.
(23) Che, C. M.; Herbstein, F. M.; Schaefer, W. P.; Marsh, R. E.; Gray, H. B. *J. Am. Chem. Soc.* **1983**, *105*, 4604.
(24) Clark, R. J. H.; Kurmoo, M.; Dawes, H. M.; Hursthouse, M. B. *Inorg. Chem.* **1986**, *25*, 409.
(25) Alexander, K. A.; Bryan, S. A.; Fronczek, F. R.; Fultz, W. C.; Rheingold, A. L.; Roundhill, D. M.; Stein, P.; Watkins, S. F. *Inorg. Chem.* **1985**, *24*, 2803.
(26) Baxter, L. A. M.; Heath, G. A.; Raptis, R. G.; Willis, A. C. *J. Am. Chem. Soc.* **1992**, *114*, 6944.
(27) Donath, H.; Avtomonov, E. V.; Sarraje, I.; von Dahlen, K. H.; El-Essawi, M.; Lorberth, J.; Seo, B. S. *J. Organomet. Chem.* **1998**, *559*, 191.
(28) Uttecht, J. G.; Näther, C.; Preetz, W. *Z. Anorg. Allg. Chem.* **2002**, *628*, 2847.
(29) Drews, H. H.; Preetz, W. *Z. Anorg. Allg. Chem.* **1997**, *623*, 509.
(30) Che, C. M.; Lee, W. M.; Mak, T. C. W.; Gray, H. B. *J. Am. Chem. Soc.* **1986**, *108*, 4446.
(31) Bennett, M. A.; Bhargava, S. K.; Boas, J. F.; Boeré, R. T.; Bond, A. M.; Edwards, A. J.; Guo, S. X.; Hammerl, A.; Pilbrow, J. R.; Privér, S. H.; Schwerdtfeger, P. To be submitted for publication.

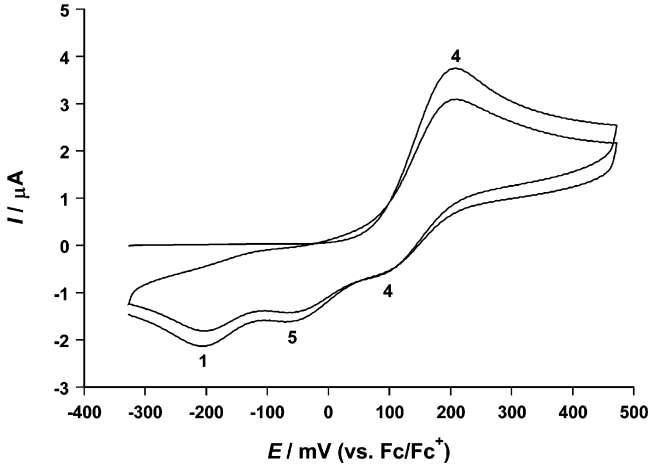

Figure 5. Cyclic voltammogram for oxidation of 1.0 mM solution of complex **1** at a 1 mm diameter GC working electrode in dichloromethane (0.1 M Bu_4NPF_6) at a scan rate of 500 mV s^{-1}.

and is also accessible by the action of very mild chemical oxidants such as Fc^+.[31] In contrast, very powerful chemical oxidants would be required to reach oxidation states beyond the mixed-valent Pt_2(II,III) species. Iodine would certainly not be a sufficiently powerful oxidizing agent to doubly oxidize **2** to $\mathbf{2}^{2+}$ but is predicted to enable $\mathbf{2}^+$ to be formed along with I^- and hence enable the lantern structured [Pt_2I_2-(μ-κAs,κC-C_6H_3-5-Me-2-$AsPh_2$)$_4$] complex **5** to be formed by a reaction sequence of the kind presented in eqs 3a−c.

$$[Pt_2(\mu\text{-}\kappa As,\kappa C\text{-}C_6H_3\text{-}5\text{-}Me\text{-}2\text{-}AsPh_2)_4] + {}^1/_2I_2 \rightleftharpoons [Pt_2(\mu\text{-}\kappa As,\kappa C\text{-}C_6H_3\text{-}5\text{-}Me\text{-}2\text{-}AsPh_2)_4]^+ + I^- \quad (3a)$$

$$[Pt_2(\mu\text{-}\kappa As,\kappa C\text{-}C_6H_3\text{-}5\text{-}Me\text{-}2\text{-}AsPh_2)_4]^+ + I^- \rightarrow [Pt_2I(\mu\text{-}\kappa As,\kappa C\text{-}C_6H_3\text{-}5\text{-}Me\text{-}2\text{-}AsPh_2)_4] \quad (3b)$$

$$2[Pt_2I(\mu\text{-}\kappa As,\kappa C\text{-}C_6H_3\text{-}5\text{-}Me\text{-}2\text{-}AsPh_2)_4] \rightarrow [Pt_2(\mu\text{-}\kappa As,\kappa C\text{-}C_6H_3\text{-}5\text{-}Me\text{-}2\text{-}AsPh_2)_4] + [Pt_2I_2(\mu\text{-}\kappa As,\kappa C\text{-}C_6H_3\text{-}5\text{-}Me\text{-}2\text{-}AsPh_2)_4] \quad (3c)$$

The failure to detect the proposed intermediate [Pt_2I(μ-κAs,κC-C_6H_3-5-Me-2-$AsPh_2$)$_4$] is consistent with rapid disproportionation (eq 3c). Overall, this series of reactions corresponds to a net oxidative addition (eq 4).

$$[Pt_2(\mu\text{-}\kappa As,\kappa C\text{-}C_6H_3\text{-}5\text{-}Me\text{-}2\text{-}AsPh_2)_4] + I_2 \rightleftharpoons [Pt_2I_2(\mu\text{-}\kappa As,\kappa C\text{-}C_6H_3\text{-}5\text{-}Me\text{-}2\text{-}AsPh_2)_4] \quad (4)$$

Electrochemical Oxidation of [Pt_2(κ^2As,C-C_6H_3-5-Me-2-$AsPh_2$)$_2$(μ-κAs,κC-C_6H_3-5-Me-2-$AsPh_2$)$_2$] (1). Crystals of **1** were manually separated from the mixture of **1** and **2** to provide low concentrations of pure **1**. A cyclic voltammogram of **1** (Figure 5) at a scan rate of 500 mV s^{-1} contains an oxidation peak at about 200 mV, which is approximately 300 mV more positive than that for the $\mathbf{2} \rightarrow \mathbf{2}^+$ process. Three reduction processes at about 100, −60, and −200 mV (vs Fc/Fc^+), labeled 4, 5, and 1, respectively, also are observed in the reverse scan. Thus, it is proposed that complex **1** is initially oxidized to $\mathbf{1}^+$, which, in a two-step process, forms complex $\mathbf{2}^+$. In support of this hypothesis, it is noted that the potential of reduction peak 1 is very similar to the reduction peak potential of complex $\mathbf{2}^+$ and that in multicycling experiments with **1**, the process now assigned to the reaction $\mathbf{2}^{0/+}$ has the same characteristics as those detected with bulk solutions of pure **2**. Additionally, after a one-electron bulk oxidative electrolysis at a controlled potential of +400 mV vs Fc/Fc^+, cyclic voltammograms have the same number of peaks and same peak potentials to those formed after bulk electrolysis of **2**. That is, processes 4 and 5 disappear with only reversible process $\mathbf{2}^{+/0}$ being detected (now reductive) along with oxidative processes 2 and 3 at very positive potentials (see Figure 4).

When the scan rate is increased to 10 V s^{-1}, the oxidation process is chemically reversible (coupled homogeneous chemical isomerization reactions are now insignificant). The $E_f{}^0$ value of 150 ± 5 mV obtained at fast scan rates from the average of the oxidation and reduction peak potentials confirms that complex **1** is thermodynamically more difficult to oxidize than **2** by about 300 mV. A theoretical rationalization of the differences in potential will be presented in future work.[31]

The ladder square scheme[32−34] mechanism, summarized in eq 5, is consistent with the cyclic voltammetry and bulk electrolysis experiments

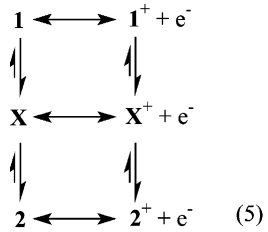

(5)

where **X** and $\mathbf{X}^+$ are intermediates of unknown structure. Simulations, rotating disk electrode, and electron paramagnetic resonance data in support of eq 5 will be presented in a forthcoming paper.[31] This scheme implies that chemical oxidation of half-lantern **1** will generate $\mathbf{2}^+$, thus explaining why the overall oxidative additive reactions commencing with either **1** or **2** or mixtures produce dihalodiplatinum(III) complexes containing the lantern structure present in $\mathbf{2}^+$.

Complex **1** also exhibits a second chemically irreversible oxidation process at 1500 ± 5 mV at a scan rate of 500 mV s^{-1}. In view of the close proximity to the solvent limit, the details of the second process could not be elucidated, but it probably represents the oxidation of $\mathbf{1}^+/\mathbf{X}^+/\mathbf{2}^+$ to a transient Pt_2(III,III) dinuclear or other electroactive complexes as has been assumed to occur when **2** is oxidized at very positive potentials (see eq 2). Like **2**, **1** is not detected to undergo reduction under voltammetric conditions, even at potentials as negative as −3000 mV.

Electrochemical Reduction of [Pt_2Cl_2(μ-κAs,κC-C_6H_3-5-Me-2-$AsPh_2$)$_4$] (3). A cyclic voltammogram of complex

(32) Bond, A. M.; Keene, F. R.; Rumble, N. W.; Searle, G. H.; Snow, M. R. *Inorg. Chem.* **1978**, *17*, 2847.
(33) Bond, A. M.; Hambley, T. W.; Snow, M. R. *Inorg. Chem.* **1985**, *24*, 1920.
(34) Evans, D. H. *Chem. Rev.* **1990**, *90*, 739.

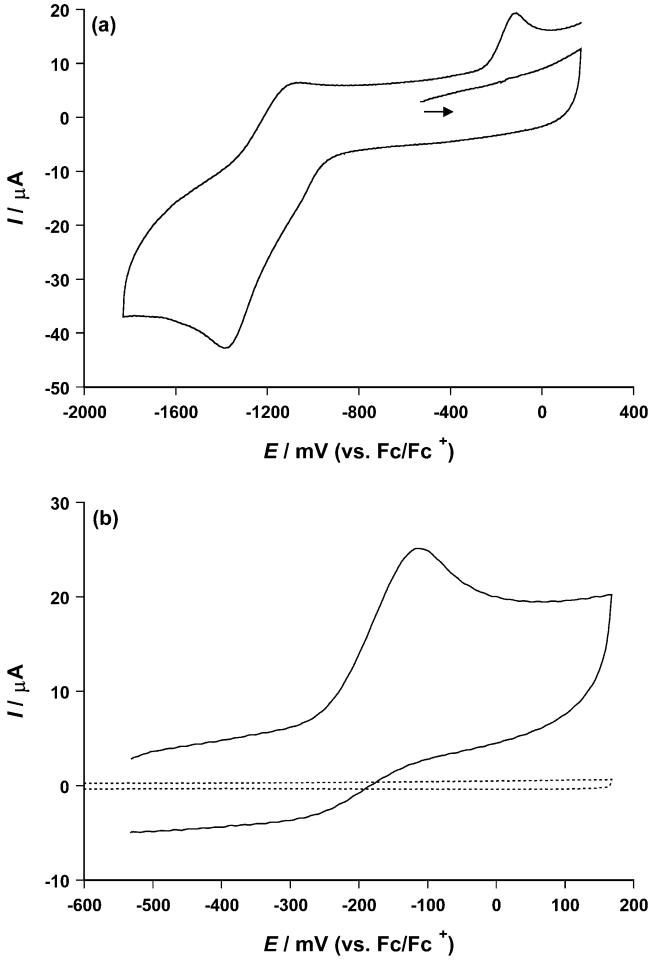

Figure 6. Cyclic voltammograms obtained at a scan rate of 1000 mV s^{-1} with a 3 mm diameter GC working electrode for (a) reduction of 0.25 mM **3** in dichloromethane (0.1 M Bu_4NPF_6) over a wide potential range and (b) cyclic voltammogram obtained in the oxidation potential range before (···) and after (—) reductive bulk electrolysis at −1500 mV (vs Fc/Fc^+) with a platinum basket electrode.

3 (Figure 6a) at a scan rate of 1000 mV s^{-1} exhibits a reduction peak at −1390 mV vs Fc/Fc^+ along with a shoulder at less negative potential. When the scan direction is reversed, an oxidation peak is observed at −115 mV, which is attributed to the oxidation of one or more reduction products since no oxidation process is detected when the potential is initially scanned in the positive direction (Figure 6a). However, the nature of the reductive component of the cyclic voltammetry depends very much on the number of cycles of the potential (Figure S1), the scan rate (compare Figure 6a and S1), and the electrode surface (Figure S2), implying that the reduction mechanism is complex. In contrast, the oxidative process coupled to the reduction step is essentially independent of electrode surface (Figure S2). No evidence for further reduction was detected in the negative potential range (−1500 mV to solvent limit) at glasy carbon (−3000 mV), platinum, or gold electrodes.

The overall results obtained by bulk electrolysis are readily interpreted. Cyclic voltammetric measurements made after bulk electrolysis revealed that the chemically irreversible oxidation process detected on reverse scans prior to bulk

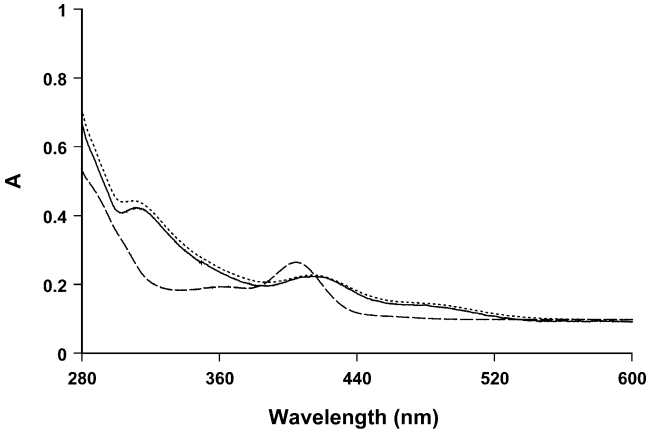

Figure 7. Electronic spectra of 0.25 mM complex **3** in dichloromethane (0.1 M Bu_4NPF_6) before electrolysis (—), after reductive electrolysis at −1500 mV (- -), and after oxidative electrolysis at +70 mV (···).

electrolysis (Figure 6a) was now present as a primary oxidation process (Figure 6b).

Oxidative bulk electrolysis of the reduced species at a potential of 70 mV vs Fc/Fc^+ re-formed complex **3**; voltammograms obtained before and after the bulk electrolysis reductive−oxidative sequence were very similar (8% loss of complex **3** estimated). However, despite the inherent complexity of the reaction scheme implied by the voltammetric measurements, on the synthetic (bulk electrolysis) time scale the reduction−oxidation cycle is close to chemically reversible (loss of less than 10% of complex **3** detected per cycle on the basis of voltammetric evidence) and corresponds to eq 6. The electrochemical data are consistent with the observation that chemical reduction of **3** with zinc dust gives pure **2** (complete absence of **1**).

$$[Pt_2Cl_2(\mu\text{-}\kappa As,\kappa C\text{-}C_6H_3\text{-}5\text{-}Me\text{-}2\text{-}AsPh_2)_4] + 2e^- \rightleftharpoons [Pt_2(\mu\text{-}\kappa As,\kappa C\text{-}C_6H_3\text{-}5\text{-}Me\text{-}2\text{-}AsPh_2)_4] + 2Cl^- \quad (6)$$

In situ spectroelectrochemical studies undertaken at a platinum gauze electrode are completely consistent with eq 6. The electronic spectrum of the reduction product (Figure 7) has absorption bands at 405 and 360 nm and closely resembles that of complex **2**. Moreover, oxidation at 70 mV vs Fc/Fc^+ leads to close to 100% recovery of the initial spectrum for complex **3**.

Neither reduction nor oxidation are believed to occur by a single-step, two-electron transfer. Rather, the data imply that one-electron intermediates are involved and that these do not need to be the same for the reduction and oxidation directions of eq 6. It is known that the oxidation of complex **2** in the absence of chloride produces $\mathbf{2}^+$ as a stable entity. In the presence of 2 equiv of halide (Cl^- and Br^-), the reversible cyclic voltammogram for the $\mathbf{2}^{0/+}$ process (Figure 3) becomes an irreversible two-electron oxidative process with all the characteristics noted after bulk reduction of **3** to **2** (eq 6, Figure 6b). Consequently, oxidation in the presence of Cl^- is assumed to be modified so as to occur via an ECE type reaction scheme for which a plausible representative example is given in eqs 7a−c.

$$[Pt_2(\mu\text{-}\kappa As,\kappa C\text{-}C_6H_3\text{-}5\text{-}Me\text{-}2\text{-}AsPh_2)_4] \rightleftharpoons [Pt_2(\mu\text{-}\kappa As,\kappa C\text{-}C_6H_3\text{-}5\text{-}Me\text{-}2\text{-}AsPh_2)_4]^+ + e^-(E) \quad (7a)$$

$$[Pt_2(\mu\text{-}\kappa As,\kappa C\text{-}C_6H_3\text{-}5\text{-}Me\text{-}2\text{-}AsPh_2)_4]^+ + 2Cl^- \rightleftharpoons [Pt_2Cl_2(\mu\text{-}\kappa As,\kappa C\text{-}C_6H_3\text{-}5\text{-}Me\text{-}2\text{-}AsPh_2)_4]^-(C) \quad (7b)$$

$$[Pt_2Cl_2(\mu\text{-}\kappa As,\kappa C\text{-}C_6H_3\text{-}5\text{-}Me\text{-}2\text{-}AsPh_2)_4]^- \rightleftharpoons [Pt_2Cl_2(\mu\text{-}\kappa As,\kappa C\text{-}C_6H_3\text{-}5\text{-}Me\text{-}2\text{-}AsPh_2)_4] + e^-(E) \quad (7c)$$

Numerous disproportionation and related second-order processes and other intermediates also could give rise to the final product (complex **3**). The reduction process also may be postulated to proceed via ECE type schemes. Irrespective of the details of the mechanism, in the presence of a ligand such as Cl^-, an overall two-electron oxidative addition−reductive elimination sequence is available, whereas in the absence of a coordinating ligand, one-electron oxidized $\mathbf{2}^+$ is detected as a stable compound.[31]

Discussion

Although there are many examples of quadruply bridged diplatinum(II) and diplatinum(III) complexes with a lantern geometry,[8,9] complexes **2**−**8** represent the first examples containing a tertiary arsine. Moreover, there is only one previous example of a diplatinum(III) complex of this type containing a carbon-donor ligand, $[Pt_2Cl_2(\mu\text{-}\kappa O,\kappa O\text{-}O_2CMe)_2(\mu\text{-}\kappa O,\kappa C\text{-}CH_2CO_2)_2]^{2-}$.[35]

The isolation of the dinuclear complexes **1** and **2** rather than a mononuclear species $[Pt(\kappa^2 As,C\text{-}C_6H_3\text{-}5\text{-}Me\text{-}2\text{-}AsPh_2)_2]$ and the conversion of **1** into the lantern dimer **2** demonstrate that the bridging $\mu\text{-}\kappa As,\kappa C$-mode is favored over κ^2-binding for ortho-metalated arylarsines. Isomerization from $\kappa^2 As,C$- to $\mu\text{-}\kappa As,\kappa C$-binding requires dissociation of the Pt−As bond; this process evidently occurs more readily than that of the corresponding Pt−P bond, reflecting the weaker Pt−As interaction and the greater size of arsenic compared with phosphorus.

There is considerable similarity in the chemistry and structures between the platinum complexes of $\mu\text{-}\kappa As,\kappa C\text{-}C_6H_3\text{-}5\text{-}Me\text{-}2\text{-}AsPh_2$ and those containing diarylformamidinato (DArF) ligands. For example, the initially formed half-lantern dinuclear complex $Pt_2(\kappa^2 N,N\text{-}DArF)_2(\mu\text{-}\kappa N,\kappa N\text{-}DArF)_2$ isomerizes on heating to the lantern structure, analogous to complexes **1** and **2,** respectively.[36] The corresponding dichlorodiplatinum(III) and Pt_2(II,III) mixed-valent complexes have also been prepared.[36,37]

The bond lengths to the axial ligands in complexes **3**−**9** clearly show that the Pt−Pt bond exerts a strong trans-influence. Moreover, the effects of different axial ligands are reflected both in the Pt−Pt distances and in the values of $^3J_{Pt-H}$ (^{195}Pt coupling to the ortho proton). The longest Pt−Pt separation (**6**, X = CN) corresponds to the largest value of $^3J_{Pt-H}$, and the shorter Pt−Pt distances (**9**, X = F; **3**, X= Cl) correspond with smaller values of $^3J_{Pt-H}$. In this limited series, the correspondence is not exact, e.g., the value of $^3J_{Pt-H}$ for X = NCO (**8**) is higher and that of X = Cl (**3**) is lower than the values that would be expected on the basis of the Pt−Pt separations. The magnitudes of $^3J_{Pt-H}$ fall in the order X = CN > I > Br > NCS > NCO > Cl > F, which is similar to, though does not correspond exactly with, orders of trans-influence based on, for example, ν(PtH) and $^1J_{Pt-H}$ in *trans*-$[PtHX(PR_3)_2]$, $^1J_{Pt-P}$ in [PtXMe(dppe)], and $^2J_{Pt-H}$ in methylplatinum(II) complexes.[14,38] Since the coupling constants in these cases are known to be positive[39,40] and decrease with increasing trans-influence, it seems likely that $^3J_{Pt-H}$ in complexes **2**−**9** is negative, as is also the case for $^3J_{P-H}$ (cis) in methylplatinum(II) complexes.[40]

We have so far been unable to isolate mixed-valent Pt_2(II,III) species of the type $[Pt_2X(\mu\text{-}\kappa As,\kappa C\text{-}C_6H_3\text{-}5\text{-}Me\text{-}2\text{-}AsPh_2)_4]$ (X = anionic ligand). Although complexes of this type are well-known with pop and other bridging ligands, such as dithioacetate, the pop compounds are reported to disproportionate readily in aqueous solution.[9b,24] Such Pt_2(II,III) halide bridged intermediates are very likely to be associated with the electrochemistry of **3**. Interestingly, the electrochemical studies demonstrate that the mixed-valence cation $[Pt_2(\mu\text{-}\kappa As,\kappa C\text{-}C_6H_3\text{-}5\text{-}Me\text{-}2\text{-}AsPh_2)_4]^+$ is stable and long-lived in solution in the absence of halide ion; this may provide access to a wider range of diplatinum(III) complexes containing the As−C bridging system.

The electrochemical data enable the synthetic results in this work to be fully rationalized, in particular, the exclusive formation of the complexes **3**−**5** from oxidation of complex **1** or **2** with halogen (X_2). In the case of the oxidation of **2**, no structural change need occur with respect to the Pt bonding after an initial one-electron oxidation by X_2 to generate $\mathbf{2}^+$ and X^-. These products of the initial redox process can then react with each other to produce a halide adduct of the one-electron-oxidized product, as shown in eqs 3a and 3b, with X replacing I.

The intermediate $[Pt_2X(\mu\text{-}\kappa As,\kappa C\text{-}C_6H_3\text{-}5\text{-}Me\text{-}2\text{-}AsPh_2)_4]$ may disproportionate, as shown in eq 3c for X = I or, in the case of the stronger oxidant chlorine, could undergo further oxidation to give directly the final oxidative addition product **3** (eq 8).

$$[Pt_2Cl(\mu\text{-}\kappa As,\kappa C\text{-}C_6H_3\text{-}5\text{-}Me\text{-}2\text{-}AsPh_2)_4] + {}^1/_2Cl_2 \rightarrow [Pt_2Cl_2(\mu\text{-}\kappa As,\kappa C\text{-}C_6H_3\text{-}5\text{-}Me\text{-}2\text{-}AsPh_2)_4] \quad (8)$$

In the case of oxidation of **1**, according to the electrochemical studies, isomerization of initially formed $\mathbf{1}^+$ to $\mathbf{2}^+$ provides the opportunity to achieve the structural change needed to ultimately give **3** (eqs 9a−c, then as in eq 3 or 7).

(35) Yamaguchi, J.; Sasaki, Y.; Ito, T. *J. Am. Chem. Soc.* **1990**, *112*, 4038.
(36) Cotton, F. A.; Matonic, J. H.; Murillo, C. A. *Inorg. Chem.* **1996**, *35*, 498.
(37) Cotton, F. A.; Matonic, J. H.; Murillo, C. A. *Inorg. Chim. Acta* **1997**, *264*, 61.
(38) Appleton, T. G.; Bennett, M. A. *Inorg. Chem.* **1978**, *17*, 738.
(39) (a) McFarlane, W. *Chem. Commun.* **1967**, 772. (b) Dean, R. R.; Green, J. C. *J. Chem. Soc. A* **1968**, 3047.
(40) Bennett, M. A.; Bramley, R.; Tomkins, J. B. *J. Chem. Soc., Dalton Trans.* **1973**, 166.

$$[Pt_2(\kappa^2As,C\text{-}C_6H_3\text{-}5\text{-}Me\text{-}2\text{-}AsPh_2)_2(\mu\text{-}\kappa As,\kappa C\text{-}C_6H_3\text{-}5\text{-}Me\text{-}2\text{-}AsPh_2)_2] + {}^1/_2X_2 \rightleftharpoons [Pt_2(\kappa^2As,C\text{-}C_6H_3\text{-}5\text{-}Me\text{-}2\text{-}AsPh_2)_2(\mu\text{-}\kappa As,\kappa C\text{-}C_6H_3\text{-}5\text{-}Me\text{-}2\text{-}AsPh_2)_2]^+ + X^- \quad (9a)$$

$$[Pt_2(\kappa^2As,C\text{-}C_6H_3\text{-}5\text{-}Me\text{-}2\text{-}AsPh_2)_2(\mu\text{-}\kappa As,\kappa C\text{-}C_6H_3\text{-}5\text{-}Me\text{-}2\text{-}AsPh_2)_2]^+ \rightarrow [Pt_2(\mu\text{-}\kappa As,\kappa C\text{-}C_6H_3\text{-}5\text{-}Me\text{-}2\text{-}AsPh_2)_4]^+ \text{ (via intermediate)} \quad (9b)$$

$$[Pt_2(\mu\text{-}\kappa As,\kappa C\text{-}C_6H_3\text{-}5\text{-}Me\text{-}2\text{-}AsPh_2)_4]^+ + X^- \rightleftharpoons [Pt_2X(\mu\text{-}\kappa As,\kappa C\text{-}C_6H_3\text{-}5\text{-}Me\text{-}2\text{-}AsPh_2)_4] \quad (9c)$$

According to the electrochemical data, reduction of **3** can occur without the need for a structural change around the Pt core in any of the intermediates to give finally **2** and X^-. The fact that chemical reduction of **3** with zinc dust produces isomerically pure **2** also is therefore explained on the basis of the electrochemical results.

Although oxidative additions to dinuclear metal complexes have attracted much attention, little is known about their mechanism.[41,42] The present work indicates that the apparent two-electron oxidation by halogens involves one-electron changes, at least in the system studied. The fact that complex **2** is oxidized more readily than **1** can be correlated with the shorter metal−metal separation in the former, which allows formation of the stabilizing $5d^7-5d^7$ interaction.

Conclusions

In this study, we have prepared novel dinuclear Pt(II) and Pt(III) complexes containing cyclometalated tertiary arsine ligands, including the first fully characterized example of a difluoro complex of diplatinum(III). Two isomers, $[Pt_2(\kappa^2As,C\text{-}C_6H_3\text{-}5\text{-}Me\text{-}2\text{-}AsPh_2)_2(\mu\text{-}\kappa As,\kappa C\text{-}C_6H_3\text{-}5\text{-}Me\text{-}2\text{-}AsPh_2)_2]$ and $[Pt_2(\mu\text{-}\kappa As,\kappa C\text{-}C_6H_3\text{-}5\text{-}Me\text{-}2\text{-}AsPh_2)_4]$, have been structurally characterized in the case of the Pt(II) oxidation state, and the spontaneous isomerization from κ^2As,C- to $\mu\text{-}\kappa As,\kappa C$-binding mode was observed. Conversion to this binding mode is promoted by heat, chemical, or electrochemical oxidation, demonstrating that the lantern configuration is thermodynamically favored. Electrochemical studies of the oxidation of $[Pt_2(\mu\text{-}\kappa As,\kappa C\text{-}C_6H_3\text{-}5\text{-}Me\text{-}2\text{-}AsPh_2)_4]$ and the reduction of $[Pt_2Cl_2(\mu\text{-}\kappa As,\kappa C\text{-}C_6H_3\text{-}5\text{-}Me\text{-}2\text{-}AsPh_2)_4]$ provide insights into the mechanisms associated with oxidative addition and reductive elimination of dinuclear complexes. In particular, the electrochemical data implicate the presence of mixed-valent one-electron-oxidized or -reduced species as being important intermediates in the overall two-electron chemical oxidation/reduction pathways.

Experimental Section

General Comments. All experiments involving organolithium reagents were performed under an atmosphere of dry argon with use of standard Schlenk techniques. Diethyl ether, tetrahydrofuran, *n*-hexane, and toluene were dried over sodium/benzophenone, dichloromethane over calcium hydride, and methanol over 4 Å molecular sieves. ^1H NMR (200 MHz) and ^{13}C NMR (50 MHz) spectra were measured on a Varian Gemini 2000 spectrometer at room temperature in acid-free $CDCl_3$ or CD_2Cl_2. Chemical shifts (δ) are given in ppm, internally referenced to residual solvent signals (^1H, δ 5.32 for CD_2Cl_2 and δ 7.26 for $CDCl_3$; ^{13}C, δ 77.0 for $CDCl_3$); multiplicities are quoted without ^{195}Pt satellites. ^{19}F NMR (282 MHz) spectra were acquired on a Varian Unity Inova 300 spectrometer, internally referenced to $CFCl_3$. Elemental analyses were performed by the Microanalytical Unit at the Research School of Chemistry, ANU, Canberra, on samples that had been dried at 50 °C in vacuo to remove residual solvent. The carbon analyses for complexes containing nitrogen (**6**−**8**) were consistently low, perhaps due to incomplete combustion. Mass spectral data were obtained on a VG ZAB-2SEQ (FAB with NOPE as matrix) or HP 5970 MSD (EI) spectrometer. IR spectra in the ranges 4000−400 cm^{-1} and 400−30 cm^{-1} were obtained as KBr and polythene disks, respectively, on a Perkin-Elmer Spectrum 2000 FT-spectrometer. Molecular weights were determined on a Knauer vapor pressure osmometer with ~0.2 M CH_2Cl_2 solutions at 37 °C. Melting points were measured on a Gallenkamp melting point apparatus in open glass capillaries and are uncorrected. $Me_3SiAsPh_2$,[6] 3-Br-4-IC_6H_3-Me,[43] 2-$BrC_6H_4AsMe_2$,[5c] $PhICl_2$,[44] $[PtCl_2(SEt_2)_2]$,[45] and $[PdCl_2(NCMe)_2]$[46] were prepared by literature methods, and the ligand 2-Br-4-$MeC_6H_3AsPh_2$[7] was prepared by a modified literature method, the details of which are given below.

Tetrabutylammonium hexafluorophosphate (Bu_4NPF_6) (GFS) used as the supporting electrolyte was purified according to a literature method.[47] Electrochemical data were obtained with a BAS model 100B electrochemical workstation. The auxiliary electrode was always platinum gauze. The potential of the Ag/AgCl (CH_2Cl_2, saturated LiCl) reference electrode was always calibrated against that of the ferrocene/ferrocenium (Fc/Fc^+) redox couple. The 1 mm diameter glassy carbon (GC) or platinum voltammetric working electrodes were polished and cleaned prior to use. For bulk electrolysis, the working electrode was cylindrical platinum gauze. Spectroelectrochemical studies were undertaken with a Cary 5 UV−visible-NIR spectrophotometer interfaced to a BAS model 100A electrochemistry system. A rectangular quartz cuvette (1 mm path length) was used as the electrochemical cell with a platinum gauze working electrode. All electrochemical studies were carried out at 20 ± 1 °C. Dichloromethane solutions were always purged with solvent-saturated nitrogen gas.

Crystals adequate for X-ray diffraction studies were grown by layering a dichloromethane solution of the complex with methanol (complexes **1**−**8**) or *n*-pentane (complex **9**). Selected crystal data and details of data collection and structure refinement are in Table 2. Crystals were coated in viscous oil and mounted on fine drawn glass capillaries, and data were collected at 200 K on a Nonius-Kappa CCD diffractometer using graphite-monochromated Mo Kα radiation (λ = 0.71073 Å). The data were measured by use of COLLECT;[48] the intensities of the reflections were extracted, and the data reduced by use of the computer programs Denzo and

(41) Collman, J. P.; Hegedus, L.; Norton, R.; Finke, R. G. *Principles and Applications of Organotransition Metal Chemistry*; University Science Books: Mill Valley, CA, 1987; Chapter 5, pp 306−322.
(42) Fackler, J. P., Jr. *Polyhedron* **1997**, *16*, 1.
(43) Bhargava, S. K.; Mohr, F.; Bennett, M. A.; Welling, L. L.; Willis, A. C. *Organometallics* **2000**, *19*, 5628.
(44) Lucas, H. J.; Kennedy, E. R. *Organic Synthesis*; Wiley and Sons: New York, 1955; Collect. Vol. 3, p 482.
(45) Kauffman, G. B.; Cowan, D. O. *Inorg. Synth.* **1960**, *6*, 211.
(46) Hartley, F. R.; Murray, S. G.; McAuliffe, C. A. *Inorg. Chem.* **1979**, *18*, 1394.
(47) Kissinger, P. T.; Heineman, W. R. *Laboratory Techniques in Electroanalytical Chemistry*; Marcel Dekker: New York, 1984; p 481.
(48) COLLECT Software, Nonius BV, 1997−2001.

Scalepak.[49] The structures were solved by direct methods (SIR92[50] for **1**, **2**, and **4**−**9**; SIR97[51] for **3**) and refined on *F* with use of CRYSTALS[52] or, in the case of the twinned crystal of **5**, RAELS 2000.[53] Calculations were performed with use of crystallographic software packages teXsan,[54] maXus,[55] and CRYSTALS.[52] The neutral atom scattering factors were taken from ref 56. The mass attenuation coefficients were those implemented in maXus.[55] Nonroutine aspects of X-ray crystallographic determinations of **1**−**9** are detailed in Appendix S1.

Preparations. 2-Br-4-MeC$_6$H$_3$AsPh$_2$. To a solution of 3-bromo-4-iodotoluene (13.08 g, 44.0 mmol) and [PdCl$_2$(NCMe)$_2$] (0.28 g, 1.07 mmol) in toluene (30 mL) under argon, (trimethylsilyl)-diphenylarsine (14.01 g, 46.3 mmol) was added, and the dark solution was heated to ca. 90 °C for 2 h. To the cooled mixture, chloroform (30 mL) was added, and the orange solution was washed with saturated sodium bicarbonate solution, water, and brine. The organic layer was separated and dried (MgSO$_4$), and the solvent was removed. The dark oil was chromatographed on a silica gel column and eluted with 1:1 toluene/hexanes. Removal of the solvent and recrystallization from ethanol gave white needles (14.25 g, 81%). ^{1}H NMR: δ 2.32 (s, 3H, Me), 6.72 (d, J_{H-H} = 7.7 Hz, 1H, aromatic H), 7.00 (dd, J_{H-H} = 0.9, 7.7 Hz, 1H, aromatic H), 7.43 (d, J_{H-H} = 0.9 Hz, 1H, aromatic H), 7.2−7.4 (m, 10H, aromatics). ^{13}C NMR: δ 20.8, 128.5, 128.6, 128.7, 130.0, 133.2, 133.8, 134.6, 137.9, 139.0, 140.5. EI-MS (*m*/*z*): 398 [M]$^+$. Anal. Calcd for C$_{19}$H$_{16}$AsBr: C, 57.17; H, 4.04; Br, 20.02. Found: C, 57.36; H, 4.12; Br, 20.26.

Mixture of [Pt$_2$(κ^2*As*,*C*-C$_6$H$_3$-5-Me-2-AsPh$_2$)$_2$(μ-κ*As*,κ*C*-C$_6$H$_3$-5-Me-2-AsPh$_2$)$_2$] (1) and [Pt$_2$(μ-κ*As*,κ*C*-C$_6$H$_3$-5-Me-2-AsPh$_2$)$_4$] (2). To a suspension of (2-bromo-4-methylphenyl)diphenylarsine (1.11 g, 2.55 mmol) in diethyl ether (10 mL), Bu^{n}Li (1.6 M, 1.6 mL, 2.56 mmol) was added to give a clear solution, which was stirred for 1 h during which time a white precipitate formed. The solvent was decanted from the precipitated solid, and diethyl ether (20 mL) was added. The suspension was cooled to −30 °C and treated with [PtCl$_2$(SEt$_2$)$_2$] (0.51 g, 1.14 mmol). The mixture was stirred for 30 min at −30 °C, then at room temperature overnight. The solvent was decanted from the yellow solid, which was washed with hexanes (2 × 10 mL) and MeOH (2 × 10 mL) and recrystallized from CH$_2$Cl$_2$/MeOH to give a mixture of **1** and **2** as a bright yellow−green solid (0.38 g, 40%). When the isomeric mixture was refluxed in toluene for 24 h, **1** was completely converted into **2**. ^{1}H NMR: δ 1.93 (s, 3H, Me of **1**), 1.98 (s, 3H, Me of **2**), 2.18 (s, 6H, Me of **2**), 6.2−7.5 (m, 48H, aromatics of **1** and **2**), 7.90 (s, J_{Pt-H} = 58.4 Hz, 4H, aromatic H ortho to Pt−C). Ratio **1**:**2** typically ca. 2:1. FAB-MS (*m*/*z*): 1666 [M]$^+$. Anal. Calcd for C$_{76}$H$_{64}$As$_4$Pt$_2$: C, 54.75; H, 3.87. Found: C, 54.64; H, 3.97.

[Pt$_2$Cl$_2$(μ-κ*As*,κ*C*-C$_6$H$_3$-5-Me-2-AsPh$_2$)$_4$] (3). To a solution containing a mixture of **1** and **2** (186 mg, 0.11 mmol) in CH$_2$Cl$_2$ (15 mL), iodobenzene dichloride (31 mg, 0.11 mmol) dissolved in CH$_2$Cl$_2$ (5 mL) was added, causing an immediate color change from yellow to orange. After the mixture was stirred for 10 min, the solution was evaporated to dryness, and the residue was recrystallized from CH$_2$Cl$_2$/hexanes to give **3** as an orange solid (187 mg, 96%). ^{1}H NMR: δ 2.19 (s, 12H, Me), 6.3−7.2 (m, 48H, aromatics), 8.32 (s, J_{Pt-H} = 35.0 Hz, 4H, aromatic H ortho to Pt−C). FAB-MS (*m*/*z*): 1702 [M − Cl]$^+$. IR: 203 cm^{-1} (Pt−Cl). Anal. Calcd for C$_{76}$H$_{64}$As$_4$Cl$_2$Pt$_2$: C, 52.52; H, 3.71; Cl, 4.08. Found: C, 52.04; H, 3.66; Cl, 4.15.

[Pt$_2$X$_2$(μ-κ*As*,κ*C*-C$_6$H$_3$-5-Me-2-AsPh$_2$)$_4$] (X = Br, 4; I, 5). To a solution of **2** (100 mg, 0.060 mmol) in CH$_2$Cl$_2$ (15 mL), 1 equiv of halogen in CH$_2$Cl$_2$ (5 mL) was added. The yellow solution immediately changed color and was stirred for 10 min. After removal of the solvent, the residue was recrystallized from CH$_2$Cl$_2$/hexanes to give the products in ca. 90% yield. Alternatively, **4** and **5** may be obtained by metathesis of a CH$_2$Cl$_2$ solution of **3** with an excess of LiX in MeOH.

X = Br, **4**. ^{1}H NMR: δ 2.16 (s, 12H, Me), 6.4−7.2 (m, 48H, aromatics), 8.49 (s, J_{Pt-H} = 37.9 Hz, 4H, aromatic H ortho to Pt−C). FAB-MS (*m*/*z*): 1747 [M − Br]$^+$. Anal. Calcd for C$_{76}$H$_{64}$As$_4$Br$_2$Pt$_2$: C, 49.96; H, 3.53; Br, 8.75. Found: C, 49.78; H, 3.43; Br, 8.95.

X = I, **5**. ^{1}H NMR: δ 2.12 (s, 12H, Me), 6.3−7.2 (m, 48H, aromatics), 8.90 (s, J_{Pt-H} = 42.8 Hz, 4H, aromatic H ortho to Pt−C). FAB-MS (*m*/*z*): 1792 [M − I]$^+$. Anal. Calcd for C$_{76}$H$_{64}$As$_4$I$_2$Pt$_2$: C, 47.52; H, 3.36; I, 13.21. Found: C, 47.90; H, 3.69; I, 13.21.

[Pt$_2$X$_2$(μ-κ*As*,κ*C*-C$_6$H$_3$-5-Me-2-AsPh$_2$)$_4$] (X = CN, 6; F, 9). To a solution of **3** (100 mg, 0.058 mmol) in CH$_2$Cl$_2$ (40 mL), an excess of AgX (ca. 0.2−0.3 mmol) was added. The mixture was stirred in the dark for 3 days. The pale yellow, turbid solution was filtered through Celite, hexanes added, and the solution evaporated. Complexes **6** and **9** precipitated as a pale yellow solids in yields of 90 and 72%, respectively.

X = CN, **6**. ^{1}H NMR: δ 2.23 (s, 12H, Me), 6.2−7.2 (m, 48H, aromatics), 8.60 (s, J_{Pt-H} = 46.9 Hz, 4H, aromatic H ortho to Pt−C). EI-MS (*m*/*z*): 1692 [M − CN]$^+$. IR: 2123 cm^{-1} (CN). Anal Calcd. for C$_{78}$H$_{64}$As$_4$N$_2$Pt$_2$: C, 54.49; H, 3.75; N, 1.63. Found: C, 52.79; H, 3.73; N, 1.99.

X = F, **9**. ^{1}H NMR (CD$_2$Cl$_2$): δ 2.18 (s, 12H, Me), 6.5−7.2 (m, 48H, aromatics), 8.04 (s with ^{195}Pt satellites, J_{Pt-H} = 29.4 Hz, 4H, aromatic H ortho to Pt−C bond). ^{19}F NMR (CD$_2$Cl$_2$): δ −228.6 (s with ^{195}Pt satellites, $^1J_{Pt-F}$ = 492 Hz, $^2J_{Pt-F}$ = 192 Hz). EI-MS (*m*/*z*): 1703 [M]$^+$. Anal. Found: C, 53.51; H, 3.82; F, 2.24. C$_{76}$H$_{64}$As$_4$F$_2$Pt$_2$ requires: C, 53.53; H, 3.78; F, 2.23.

[Pt$_2$X$_2$(μ-κ*As*,κ*C*-C$_6$H$_3$-5-Me-2-AsPh$_2$)$_4$] (X = NCS, 7; NCO, 8). To a solution of **3** (100 mg, 0.058 mmol) in CH$_2$Cl$_2$ (40 mL), an excess of NaX (ca. 0.3−0.4 mmol) in MeOH (20 mL) was added. The orange solution turned yellow and was stirred for 10 min. The solvent was removed in vacuo, CH$_2$Cl$_2$ (20 mL) was added, and the turbid solution was filtered through Celite. Addition of hexanes and evaporation of the solution caused **7** and **8** to precipitate as yellow solids in yields of ca. 90%.

X = NCS, **7**. ^{1}H NMR: δ 2.22 (s, 12H, Me), 6.3−7.1 (m, 48H, aromatics), 7.79 (s, J_{Pt-H} = 37.7 Hz, 4H, aromatic H ortho to Pt−C). EI-MS (*m*/*z*): 1723 [M − NCS]$^+$. IR: 2086 cm^{-1} (br, NCS). Anal. Calcd for C$_{78}$H$_{64}$As$_4$N$_2$S$_2$Pt$_2$: C, 52.53; H, 3.62; N, 1.57. Found: C, 51.21; H, 3.73; N, 1.60.

(49) Otwinowski, Z.; Minor, W. In *Methods in Enzymology*; Carter, C. W., Jr., Sweet, R. M., Eds.; Academic Press: New York, 1997; Vol. 276, pp 307−326.

(50) Altomare, A.; Cascarano, G.; Giacovazzo, C.; Guagliardi, A.; Burla, M. C.; Polidori, G.; Camalli, M. *J. Appl. Crystallogr.* **1994**, *27*, 435.

(51) Altomare, A.; Burla, M. C.; Camalli, M.; Cascarano, G. L.; Giacovazzo, C.; Guagliardi, A.; Moliterni, A. G. G.; Polidori, G.; Spagna, R. *J. Appl. Crystallogr.* **1999**, *32*, 115.

(52) Watkin, D. J.; Prout, C. K.; Carruthers, J. R.; Betteridge, P. W.; Cooper, R. I. *CRYSTALS*, Issue 11; Chemical Crystallography Laboratory: Oxford, England, 2001.

(53) Rae, A. D. *RAELS 2000: A Comprehensive Constrained Least-Square Refinement Program*; Australian National University: Canberra, ACT, Australia, 0200.

(54) *teXsan: Single-Crystal Structure Analysis Software*, Version 1.8; Molecular Structure Corp.: The Woodlands, 1997.

(55) Mackay, S.; Gilmore, C. J.; Edwards, C.; Stewart, N.; Shankland, K. *maXus Computer Program for the Solution and Refinement of Crystal Structures*; Nonius, The Netherlands, MacScience, Japan, and the University of Glasgow, 2000.

(56) *International Tables for X-ray Crystallography*; Kynoch Press: Birmingham, England, 1974; Vol. IV.

X = NCO, **8**. ^{1}H NMR: δ 2.17 (s, 12H, Me), 6.3−7.2 (m, 48H, aromatics), 7.90 (s, J_{Pt-H} = 37.4 Hz, 4H, aromatic H ortho to Pt−C). EI-MS (*m*/*z*): 1707 [M − NCO]$^+$. IR: 2186 cm^{-1} (br, NCO). Anal. Calcd for $C_{78}H_{64}As_4N_2O_2Pt_2$: C, 53.50; H, 3.68; N, 1.60. Found: C, 52.67; H, 3.58; N, 1.77.

[**Pt$_2$(*μ*-*κAs*,*κC*-C$_6$H$_4$-2-AsMe$_2$)$_4$**] **(10).** To a solution of (2-bromophenyl)dimethylarsine (0.816 g, 3.12 mmol) in diethyl ether (20 mL), Bu^{n}Li (1.6 M, 1.95 mL, 3.12 mmol) was slowly added. The clear solution became turbid and then clear again. It was stirred for 30 min and cooled to −30 °C. It was treated with [$PtCl_2(SEt_2)_2$] (0.620 g, 1.38 mmol), and the mixture was stirred for 30 min at this temperature, and then at room temperature overnight. The solvent was removed in vacuo, and CH_2Cl_2 (20 mL) was added. Filtration of the solution through Celite, addition of hexanes, and evaporation caused precipitation of **10** as a yellow−orange solid (0.743 g, 96%). ^{1}H NMR: δ 0.5−2.2 together with multiplets at δ 0.88 and 1.25 due to hexanes (m, 9H, Me and hexanes), 6.2−8.2 (m, 4H, aromatics. Anal. Found: C, 35.72; H, 3.94; mol wt 1120. $C_{32}H_{40}As_4Pt_2.0.33C_6H_{14}$ requires: C, 35.87; H, 4.17; mol wt 1115 (CH_2Cl_2).

[**Pt$_2$Cl$_2$(*μ*-*κAs*,*κC*-C$_6$H$_4$-2-AsMe$_2$)$_4$**] **(11).** To a solution of **10** (0.103 g, 0.092 mmol) in CH_2Cl_2 (3 mL), a solution of iodobenzene dichloride (26 mg, 0.095 mmol) in CH_2Cl_2 (3 mL) was added. The orange solution immediately reddened and was stirred for 15 min. The mixture was evaporated to dryness, the orange residue was dissolved in CH_2Cl_2, and hexanes were added. On evaporation of the solution, **11** precipitated as an orange solid (0.803 g, 73%). ^{1}H NMR: δ 0.5−2.2 together with multiplets at δ 0.88 and 1.25 due to hexanes (m, 9H, Me and hexanes), 6.2−8.0 (m, 4H, aromatics). Anal. Found: C, 32.69; H, 3.89; Cl, 6.08; mol. wt. 1218. $C_{32}H_{40}As_4Cl_2Pt_2$ requires: C, 32.42; H, 3.40; Cl, 5.98; mol wt 1185 (CH_2Cl_2).

Supporting Information Available: X-ray crystallographic data in CIF format for complexes **1**−**9**, appendix S1 containing details of nonroutine aspects of the X-ray crystallographic determinations of **1**−**9**, Figures S1 and S2 providing voltammograms for reduction of **3** at different electrode surfaces and scan rates, and Tables S1−S3 containing selected bond lengths. This material is available free of charge via the Internet at http://pubs.acs.org.

IC0498790